High performance reverse solar distiller with enhanced condensation and salt resistance

Dongxuan Ying, Haotian Zhang, Bingseng Wang, Nan He, Lin Li*

Key Laboratory of Ocean Energy Utilization and Energy Conservation of Ministry of Education, School of Energy and Power Engineering, Dalian University of Technology, Dalian 116024, China

Abstract: Solar interfacial evaporation represents a promising and sustainable solution for desalination. Despite its potential for high evaporation rates, the coexistence of vapor and incident light has hindered efficient freshwater collection. In this work, we propose a vapor-down harvesting reverse solar distiller (RSD) that comprises a photothermal layer, a supply water path, and a condensation chamber. Unlike conventional solar stills, the RSD enables water evaporation and photothermal conversion to occur on opposite sides, preventing mutual interference between the vapor and incident light. Furthermore, the RSD exhibits superior performance in terms of salt resistance and condensation. Remarkably, our RSD achieves a high freshwater collection rate of 1.03 kg m^{-2} h^{-1} with an impressive collection efficiency of 71%.

1. Introduction

The huge demand for freshwater due to global water scarcity and population growth has fostered an interest in developing efficient materials and systems for clean water production[1, 2]. Solar interfacial evaporation technology by localizing heat at the water-air interface has attracted significant attention and has achieved high water evaporation rates by developing light-absorbing materials such as carbon-based materials[3], metal nanomaterials[4], water absorbing materials such as hydrogels[5]. Although current evaporators can achieve high evaporation rates, they cannot collect the freshwater effectively. Conventional solar freshwater production is usually carried out in a still with a floating-structured evaporator at the bottom to produce vapor and a transparent inclined glass at the top for light transmission and condensation[6]. However, the upward diffusion of vapor interferes with the incident light, resulting in low freshwater collection efficiency[7].

To solve the problem, researchers have proposed stills with separate photothermal and evaporating surfaces, the heat generated by photothermal conversion is transferred downward to the evaporation surface, and the generated vapor continues to diffuse downward to the condensation chamber for condensation[8]. However, there are still shortcomings in the still with downward diffusion of vapor. First, the vapor needs to overcome the diffusion resistance to reach the inner surface of the chamber, and the vapor is easy to form film condensation whose thermal resistance is not conducive to latent heat release, and the air cooling on the outer wall is also detrimental to latent heat transfer (<10W m^{-2} k^{-1}). In short, excessive thermal resistance is not conducive to condensation. Secondly, the inverse distiller can only use 2D water paths, so it is not possible to use anti-salt strategies based on floating structure design[9]. The salt accumulation on the evaporating surface will affect the vapor generation and the freshwater collection. It is necessary to develop a distiller with separate photothermal and evaporating surfaces that can enhance condensation and salt resistance performance for efficient and continuous production of freshwater. Therefore, we developed a reverse solar distiller (RSD) with enhanced condensation and salt resistance, which enables efficient outdoor freshwater collection and provides a new option for solar seawater desalination.

2. Experimental procedures

2.1. Design of the RSD

The RSD consists of a selective light absorber, a condensation chamber and a water path (figure 1a). Firstly, carbon black particles, polydimethylsiloxane and curing agent were mixed and stirred in the ratio of 20:10:1 to prepare the photothermal coating, and the copper plate was covered with the photothermal coating and put into the drying oven for 2h to be made into a selective light absorber. Secondly, the condensation chamber is composed of a copper part with the size of 4 × 4 cm and multilayer nested hydrophobized micro-nanostructured (MNHM) copper surfaces inside which allow for drop condensation (figure 1b). Micro-nanostructures on copper surfaces was prepared by mechanical processing and chemical etching. The etching solution is a mixture of 2.5

*Corresponding author's e-mail: lilinnd@dlut.edu.cn

mol L^{-1} sodium hydroxide and 0.1 mol L^{-1} ammonium persulfate. Hydrophobic property of the copper was obtained by 0.5% perfluorodecyltriethoxysilane treatment for 1 h. Finally, the water path is constructed with different capillary force fabrics which has the ability to resist salt accumulation (figure 1c), the strong capillary force fabric can supply water to the evaporating surface, and the weak capillary force fabric connects the upper edge of the RSD to the bulk water. Since salt has the tendency to accumulate at the upper edge, the fabrics establish a transport bridge between the evaporating surface and the bulk water, which enhances the discharge of salt ions from the evaporation area to the bulk water, forming a closed loop (CL).

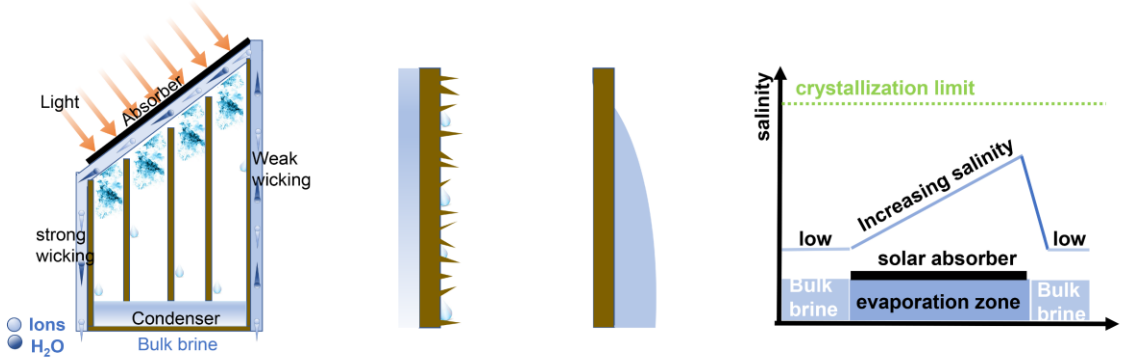

(a) Schematic diagram of the RSD (b) Condensation of MNHM (c) Salt resistance of CL

Fig.1 The design of the RSD

2.2. Characterization and measurement

Scanning electron microscope (SU8010) was used to observe the microstructure of fabric and condensation surfaces. Contact angle meter (JY-82C) was used to observe the microstructure of fabric and condensation surfaces. UV-Vis spectrophotometer (UV-3600 plus) was used to test the light absorption properties of photothermal surfaces.

2.3. Experiments for condensation

The ambient temperature of the laboratory was maintained at 20°C. The xenon lamp source (CEL-HXF300) was used to desalinate. The mass difference of the RSD before and after the experiment was recorded with a balance to calculate the yield of freshwater. Infrared camera (Ti480Pro) was used to take infrared images of the RSD. HD camera was used to observe droplet growth on copper surface.

2.4. Experiments for salt resistance

The RSD was placed in 10% brine and the xenon lamp source was used to desalinate, the yield of freshwater was measured with a balance and the evaporation surface was recorded with a camera. The salt resistance cycle test was tested for 7 days, 8h per day.

3. Results and discussion

3.1. Characterizations of the RSD

Figure 2a shows the absorption of the photothermal layer at solar wavelengths from 280 nm to 2500 nm, which can reach an average absorbance of 91%. Figure 2b shows the SEM images of two different capillary force fabrics, which have rich microscopic pore structures. The left image represents the fabric with strong wicking capacity that quickly draws in droplets in less than 50 ms, while the right image represents the fabric with weak wicking capacity that has a longer droplet penetration time. Figure 2c shows the capillary rise height of the two fabrics, compared with the weak wicking fabric, it can be seen that the strong wicking fabric can pump water to a higher position faster, showing a stronger water supply capacity. Besides, it can be seen that the treated copper transforms from a smooth surface to a surface with agglomerated protrusions. At the same time, the contact angle is changed from 89.27° to 148.92° by surface hydrophobic modification, indicating the hydrophobicity of the MNHM surface (figure 2d).

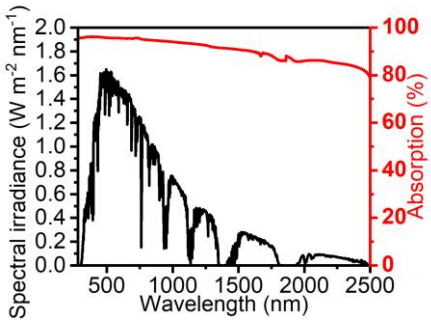

(a) Absorption spectra

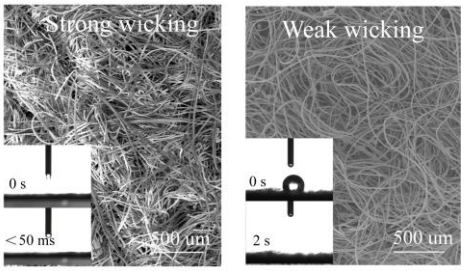

(b) SEM images of fabrics

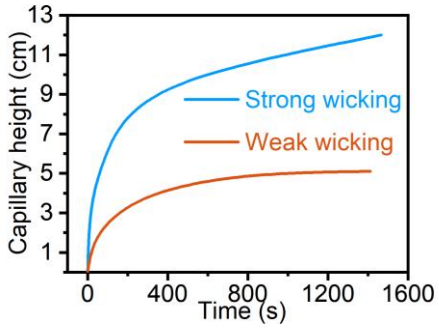

(c) Capillary height of fabrics

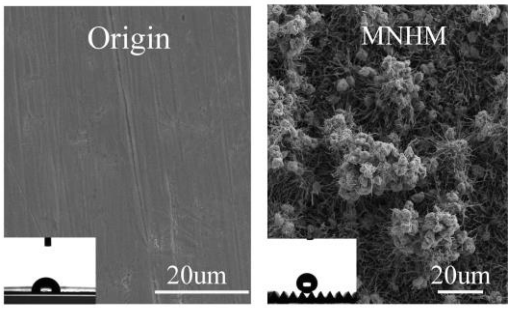

(d) SEM images of condensation surfaces

Fig.2 Characterizations of the RSD

3.2. Condensation performance of the RSD

The condensation performance of the RSD is critical to the vapor phase change and latent heat transfer. Figure 3a represents the effect of MNHM and CL on the freshwater collection rate. It can be seen that CL and MNHM contribute significantly to the increase of the RSD collection rate, with CL boosting a maximum of 0.1 kg m^{-2} h^{-1} and MNHM a maximum of 0.3 kg m^{-2} h^{-1}, and the collection rate of the RSD with MNHM and CL can reach a maximum of 1.03 kg m^{-2} h^{-1}. The collection rates both decrease with time, because the distiller starts to accumulate condensate, which results in an increase in heat transfer thermal resistance. The energy balance diagram (Figure 3b) shows that the collection process, and the heat transfer process can be analysed by the following equation:

$$q = \frac{\Delta T_{evap-cond}}{R_1} = \frac{\Delta T_{cond-amb}}{R_m} \quad (1)$$

where q is the heat flow density of condensation, $\Delta T_{evap-cond}$ is the temperature difference between vapor and the outer surface, R_1 is the equivalent thermal resistance of the diffusion layer, condensate and material, $\Delta T_{cond-amb}$ is the temperature difference between the outer surface and the external environment, $R_m = R_2$ when there is no CL cooling, and $R_m = R_{CL}$ when there is CL cooling, where R_2 is the equivalent thermal resistance of convection, conduction and radiation heat transfer from the outer surface to the air, and R_{CL} is the equivalent thermal resistance of convection, conduction and radiation heat transfer from the outer wall to the water path.

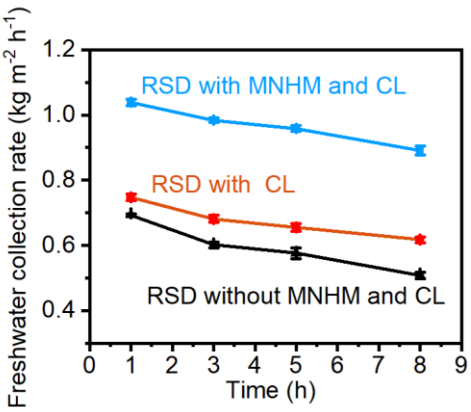

(a) The effect of MNHM and CL on the freshwater collection rate

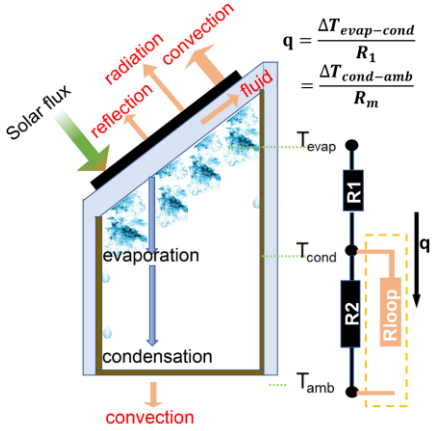

(b) Energy balance diagram of the RSD

3.3. Salt resistance performance of the RSD

When desalinating highly concentrated brine, the salt resistance of the distiller is very important for steam generation and freshwater collection. Figure 4a shows the freshwater collection rates of the RSD with CL and without CL when desalinating 10wt% brine under one sun. The freshwater collection rate of the RSD without CL is significantly lower than that of the RSD with CL, the difference between them becomes larger as the desalination progressed, from 0.21 kg m^{-2} h^{-1} at the beginning to 0.34 kg m^{-2} h^{-1} at the end. The freshwater collection rates decrease with time due to the accumulation of condensate. Figure 4b shows the evaporating surfaces of the distillers. The evaporating surface of the RSD with CL does not show obvious salt crystals, while the RSD without CL show salt accumulation from the edge of the evaporating surface until it covers the whole surface, because the ions can flow back into the bulk water along CL. To demonstrate the collection stability of the distiller, we performed seven desalination cycles (8 h each cycle) (figure 4c), resulting in a stable freshwater collection rate of 0.86 kg m^{-2} h^{-1}. Figure 4d shows that we are able to desalinate 10wt% brine, which is a bright performance among single-stage solar stills.

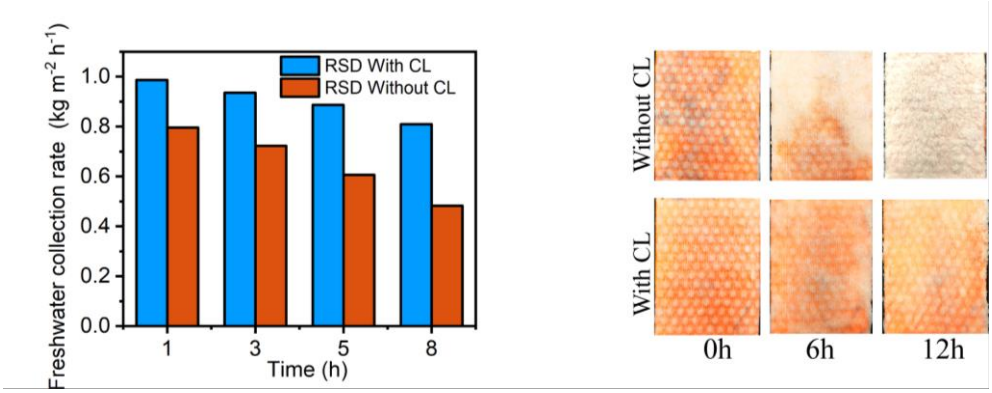

(a) The effect of CL on freshwater collection rate when desalinating 10% brine (b) Salt accumulation of evaporation surfaces

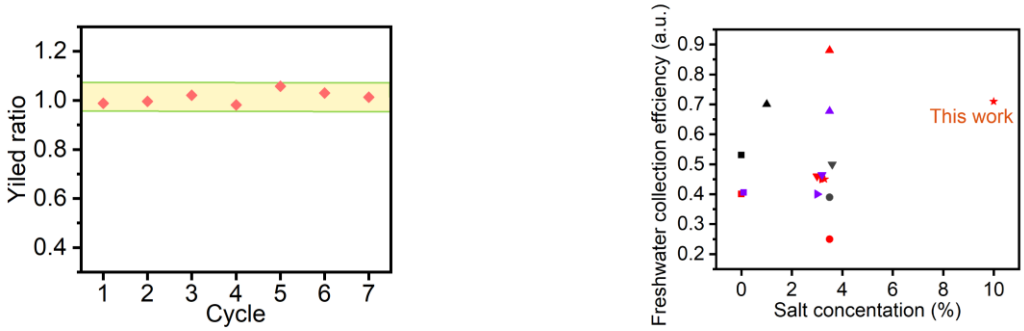

(c) Cycle tests of the RSD (d) Comparison with other solar distillers

Fig.4 Salt resistance performance of the RSD

3.4. Outdoor Performance of the RSD

To test the practical freshwater production performance of the RSD, we integrated the distiller and placed it on a foam that could float on the water. The test place was selected in the river of Dalian University of Technology (Dalian, Liaoning province, China) (Figure 5a), during a full day of testing, we recorded the actual solar radiation intensity and ambient temperature (Figure 5b). The radiation intensity ranges from 0-930 W m^{-2}, and the ambient temperature is also below 20℃. The practical yield of the freshwater is measured to be 2.7 L m^{-2} d^{-1} (figure 5c). In addition, we measured the ion concentrations in the freshwater by ICP-OES to evaluate the desalination effect of the RSD (Figure 5d), and the concentrations of K^+, Ca^{2+}, Na^+ and Mg^{2+} meet the WHO drinking water standards. The results further confirm that the RSD is a highly efficient and stable solar desalination system, proving its great value in practical water desalination.

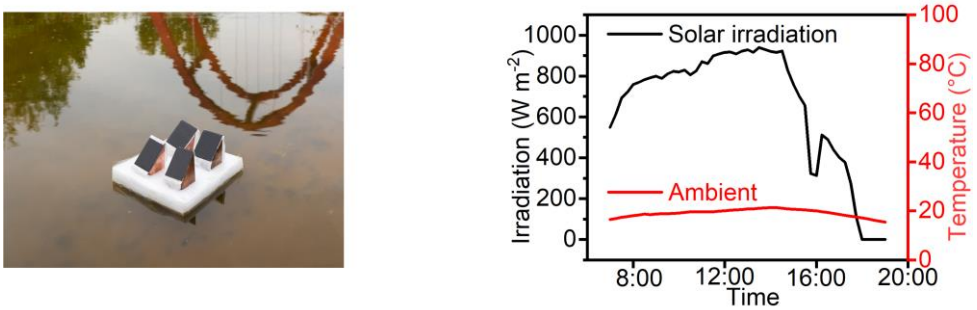

(a) Practical test images (b) Practical solar irradiation and ambient

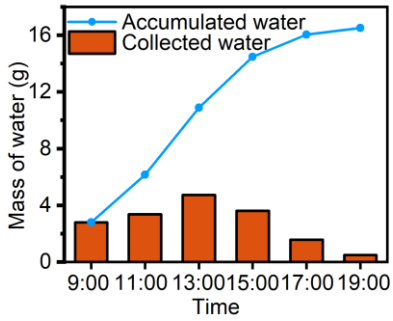

(c) Freshwater yield of practical tests

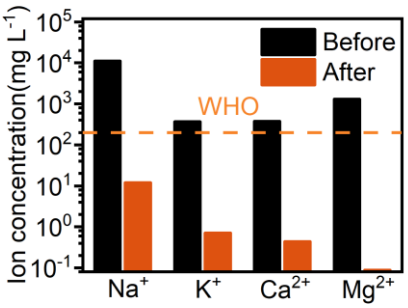

(d) Ion concentrations after desalination

Fig. 5 Outdoor Performance of the RSD

4. Conclusion

In summary, we reported a reverse solar distiller with enhanced condensation and salt resistance by the design of CL and MNHM, which can achieve a freshwater collection rate of 1.03 kg m^{-2} h^{-1} and a collection efficiency of 71%. In addition, in the practical outdoor water production test, 2.7 L m^{-2} d^{-1} can be obtained. The solar distiller has the advantages of simple structure, low cost, easy portability and high freshwater yield, which provides a new path for seawater desalination.

Acknowledgments

The authors gratefully acknowledge the financial support from the National Natural Science Foundation of China (Grant No. 52076028).

References

1. GENG Y, SUN W, YING P, et al. (2021) Bioinspired Fractal Design of Waste Biomass-Derived Solar–Thermal Materials for Highly Efficient Solar Evaporation. Advanced Functional Materials, 31(3): 2007648.
2. TAO P, NI G, SONG C, et al. (2018) Solar-driven interfacial evaporation. NATURE ENERGY, 3(12): 1031-41.
3. ZHANG H, LI L, GENG L, et al. (2023) Reduced graphene oxide/carbon nitride composite sponge for interfacial solar water evaporation and wastewater treatment. Chemosphere, 311: 137163.
4. XIAO J-K, GONG J-Z, DAI M, et al. (2023) Reduced graphene oxide/Ag nanoparticle aerogel for efficient solar water evaporation. Journal of Alloys and Compounds, 930: 167404.
5. CHEN L, WU Y, XING W, et al. (2023) Mechanically robust composite hydrogels for high performance solar driven interface evaporation. Chemical Engineering Science, 267: 118330.
6. HUSSEN H M, YOUNES M M, ALAWEE W H, et al. (2023) An experimental comparison study between four different designs of solar stills. Case Studies in Thermal Engineering, 44: 102841.
7. ALSHQIRATE A, AWAD A S, AL ALAWIN A, et al. (2023) Experimental investigation of solar still productivity enhancement of distilled water by using natural fibers. Desalination, 553: 116487.
8. YAO H Z, ZHANG P P, YANG C, et al. (2021) Janus-interface engineering boosting solar steam towards high-efficiency water collection. ENERGY & ENVIRONMENTAL SCIENCE, 14(10): 5330-8.
9. HOU X, SUN H, DONG F, et al. (2023) 3D carbonized grooved straw with efficient evaporation and salt resistance for solar steam generation. Chemosphere, 315: 137732.